ChemInform Abstract: Supported Metal Clusters: Synthesis, Structure, and Catalysis

ARTICLE *in* CHEMINFORM · AUGUST 2010

Impact Factor: 0.74 · DOI: 10.1021/cr00035a003

1 AUTHOR:

Bruce C Gates
University of California, Davis
596 PUBLICATIONS **14,511** CITATIONS

SEE PROFILE

Supported Metal Clusters: Synthesis, Structure, and Catalysis

B. C. Gates

Department of Chemical Engineering and Materials Science, University of California, Davis, California 95616

Received December 2, 1994 (Revised Manuscript Received March 7, 1995)

Contents

Supported Metal Catalysts

Metals are among the most important catalysts, being used on a large scale for refining of petroleum, conversion of automobile exhaust, hydrogenation of carbon monoxide, hydrogenation of fats, and many other processes. The metal is often expensive and may constitute only about 1 wt % of the catalytic material, being applied in a finely dispersed form as particles on a high-area porous metal oxide support (carrier).[1–5] The smaller the metal particles, the larger the fraction of the metal atoms that are exposed at surfaces, where they are accessible to reactant molecules and available for catalysis.

Supported metal catalysts are typically made by impregnation of a porous support (e.g., γ-Al_2O_3) with an aqueous solution of a metal salt (e.g., tetraammineplatinum chloride), followed by heating in air (calcining) and reduction in hydrogen.[1] The resultant structures typically consist of metal particles distributed over the internal surface of the support. Because most support surfaces are structurally nonuniform and because supported metal particles are nonuniform in size and shape and too small to be characterized precisely, the structures of supported metal catalysts are not well understood.

The average metal particle size is usually determined on the basis of the dispersion (fraction of metal atoms exposed) measured by titration of the metal surface sites by hydrogen or CO chemisorption.[5] Complementary measurements are made with transmission electron microscopy and extended X-ray absorption fine structure (EXAFS) spectroscopy.[3] With dispersion data, it is possible to determine the rate of a catalytic reaction per exposed surface metal atom, referred to as a turnover frequency or a turnover rate.[4,5]

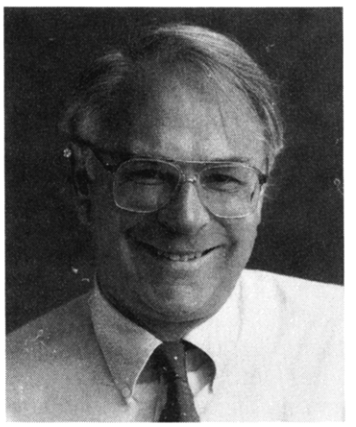

B. C. Gates is a professor in the Department of Chemical Engineering and Materials Science at the University of California at Davis, which he joined after being on the faculty of the University of Delaware for more than 20 years. Gates's research group is active in synthesis, physical characterization, and performance investigations of catalysts including supported metals and metal clusters, zeolites, and solid superacids. Gates is an editor of *Advances in Catalysis*.

Table 1. Some Properties of Idealized Platinum Clusters and Crystallites in Highly Dispersed Catalysts, as Represented by Poltorak and Boronin[6]

crystallite edge			
number of atoms	length, Å	fraction of atoms on surface	total number of atoms in crystallite
2	5.50	1.00	6
3	8.95	0.95	19
4	11.00	0.87	44
5	13.75	0.78	85
6	16.50	0.70	146

The structures of very small supported metal particles are not well known, and the particles have often been modeled as crystallites having the symmetries of bulk metals (Table 1).[6] For example, a 6-atom platinum particle is represented as an octahedron with an edge length of about 5.5 Å and a dispersion of 1. A 20-atom platinum particle with the assumed structure has an edge length of about 10 Å and a dispersion still barely distinguishable from 1. Thus metal dispersions that are determined by chemisorption measurements to be virtually unity indicate metal particles about 10 Å in size or smaller.[7]

Boudart[2] classified supported metals into three categories according to particle size, as follows:

(1) Metal particles larger than about 50 Å, which have surface structures resembling those of chunks of the bulk metal. These particles expose a number of different crystal faces with a distribution that is more or less independent of the particle size. For example, a catalyst used industrially for selective oxidation of ethylene to give ethylene oxide is silver

0009-2665/95/0795-0511$15.50/0

supported on α-Al_2O_3 (Ag/α-Al_2O_3). The silver particles are typically roughly 1 μm in size, orders of magnitude larger than the particles in more typical supported metal catalysts.

(2) Supported metal particles in the size range 10–50 Å, which, at least until recently, have been regarded as the ones of most interest because changes in the particle size lead to significant changes in properties for many catalytic reactions. There is an extensive literature of such catalysts.[7] Examples include Pt/Al_2O_3, $Re-Pt/Al_2O_3$, and $Ir-Pt/Al_2O_3$, which are used for reforming of gasoline-range hydrocarbons.[3]

(3) Supported metal particles with diameters <10 Å, which are henceforth referred to as clusters to distinguish them from the larger particles (or crystallites). Supported metal clusters were barely mentioned in Boudart's 1985 review[2] because only little was known about them then. Now such supported clusters are rapidly gaining attention because methods have been developed to prepare and characterize them and because a catalyst incorporating such clusters (platinum in the pores of LTL zeolite, Pt/LTL zeolite) has found industrial application for selective reforming of naphtha to give aromatics.

Supported metal clusters are the subject of this review.

Structure-Sensitive and Structure-Insensitive Reactions Catalyzed by Metals

Catalytic reactions that proceed at rates (per unit surface area of metal) that vary substantially (say, by an order of magnitude) from one (average) metal crystallite size to another are called *structure sensitive*.[4,5] Structure-sensitive reactions also proceed at substantially different rates on different crystal planes of single crystals of a metal.[4,5,8] Structure-sensitive catalytic reactions include those that involve breaking or making of C–C, N–N, or C–O bonds.[5] Examples are ammonia synthesis on iron and alkane hydrogenolysis on various transition metals; the latter reaction occurs in hydrocarbon reforming.

In contrast, many reactions, classified as *structure insensitive*,[4,5,8] proceed at rates (per unit surface area of metal) that are nearly the same (say, within a factor of 2) on particles of different sizes and on different crystal faces of a metal. Structure-insensitive catalytic reactions include those that involve breaking or making of H–H, C–H, or O–H bonds.[5] Examples are hydrogenation of alkenes and hydrogenation of aromatic hydrocarbons on various transition metals.

Structure-sensitive and structure-insensitive reactions have been diagnosed in catalysis experiments with supported metals having systematically varied average crystallite sizes or with different exposed faces of single crystals.

Molecular Metal Clusters and Supported Metal Clusters

In his 1985 review, Boudart[2] referred to a conceptual link between supported metal clusters and molecular metal clusters, citing Muetterties,[9] who in 1975 speculated that molecular metal clusters such as metal carbonyls would be found to be catalysts with novel properties. Examples of such clusters are $[Fe_3(CO)_{12}]$, $[Co_4(CO)_{12}]$, $[Os_3(CO)_{12}]$, $[Ir_4(CO)_{12}]$, and $[Pt_{15}(CO)_{30}]^{2-}$. One of Muetterties's arguments was that metal clusters have reactivities different from those of mononuclear (single-metal-atom) complexes, in part because they have neighboring metal centers, and the unique metal-ligand bonding in clusters would be expected to facilitate reactions like those catalyzed by metal surfaces but not mononuclear complexes. Muetterties recognized possibilities for catalytic hydrogenation of CO by metal carbonyl clusters; CO hydrogenation (Fischer–Tropsch synthesis) is catalyzed by many metal surfaces.

There is ample evidence of reactivities of ligand-stabilized metal clusters that require neighboring metal centers.[10,11] Furthermore, bare metal clusters (those lacking ligands) in the gas phase have reactivities that are strikingly dependent on the cluster size. For example, reactions of D_2 with iron, nickel, palladium, and platinum clusters indicate that both reaction rates and coverages of clusters with deuterium ligands depend on the metal, the charge, and the number of atoms in the cluster (the nuclearity).[12] The reactivity of gas-phase Co_4^+ for dehydrogenation of cyclohexane to give benzene is markedly different from that of cationic cobalt clusters with only one atom more or one atom less,[13] and the reactivity of Fe_4^+ for formation of benzene from smaller hydrocarbons is similarly unique.[14]

However, the practical application of gas-phase clusters as catalysts is seemingly not feasible, and the anticipation[9,15] of unique catalysis by ligand-stabilized molecular metal clusters is largely unrealized. The few examples of catalysis by metal carbonyl clusters in solution are neither very well understood nor of practical importance, at least by comparison with some examples of catalysis by mononuclear metal complexes. The prospects of catalysis by ligand-stabilized molecular metal clusters are limited because the more stable molecular clusters tend to be unreactive and the more reactive clusters, at least at the temperatures required for most catalytic reactions, are unstable. Coordinatively saturated clusters need to be activated, e.g., by removal of ligands, and because metal–metal bonds in many clusters are weaker than metal–ligand bonds, clusters may decompose before activation of a reactant can take place.

Nonetheless, the conceptual connections between molecular metal clusters and supported metal clusters, recognized by Ugo and Basset,[16] Chini,[17] Muetterties and Krause,[15] and Boudart,[2] now have a strong basis in experiment;[18] these connections are a theme of this review. For example, some of the most effective syntheses of supported metal clusters have been carried out with molecular metal clusters (metal carbonyls) as precursors. And some catalysts incorporate metal clusters so small and so nearly uniform that they may be regarded as quasi molecular in character.

Classes of Supported Metal Clusters

Numerous attempts have been made to prepare supported metal clusters < 10 Å in size with nearly uniform structures. There is now a substantial

literature of supported metal carbonyl clusters, including carbonyls of iron, cobalt, rhodium, osmium, iridium, and platinum on metal oxides. This literature has been thoroughly reviewed[18-22] and is cited only briefly here. Many of the supported metal carbonyl clusters are anions, often dispersed in ion pairs on basic metal oxide surfaces. Examples include the following clusters supported on MgO: $[HFe_3(CO)_{11}]^-$,[23] $[H_3Os_4(CO)_{12}]^-$,[24] $[HIr_4(CO)_{11}]^-$,[25] $[Ir_6(CO)_{15}]^{2-}$,[25] $[Ru_6C(CO)_{16}]^{2-}$,[26] and $[Pt_{15}(CO)_{30}]^{2-}$,[27] among many others. Examples of neutral metal carbonyl clusters dispersed molecularly on metal oxides that are neither strongly basic nor strongly acidic include $[Ir_4(CO)_{12}]$ on γ-Al_2O_3[28] and on SiO_2[29] and $[Rh_6(CO)_{16}]$ on SiO_2.[29]

The relevance of ligand-stabilized metal clusters on supports to the supported metal clusters of interest here is their role as precursors. Almost all of the preparations of nearly uniform supported metal clusters have involved decarbonylation of metal carbonyl clusters, most with robust metal frames, e.g., $[Ir_4(CO)_{12}]$. This cluster on γ-Al_2O_3, upon treatment in helium at 300 °C, gives decarbonylated clusters that are modeled as Ir_4 with a tetrahedral structure.[28] However, there are still only a few examples of supported clusters formed from metal carbonyls without destruction of the metal frame. Most attempts to prepare supported metal clusters by decarbonylation of supported metal carbonyls have led to ill-defined mixtures of mononuclear metal complexes and/or clusters and/or metallic particles; such nonuniform materials are largely ignored here.

Supported metal clusters have also been prepared from beams of size-selected gas-phase clusters impinging on planar surfaces. Thus Pt_n, where $n = 1$, 2, 3, 4, 5, or 6, have been prepared on oxidized silicon wafers and on carbon films.[30] Similarly, Pt_n and Pd_n, where $n = 1, 2, ...,$ or 15, have been prepared on Ag(110) single crystals.[31] There are still few well-defined examples of this type of material.

Supports for Metal Catalysts

Most catalyst supports have pores that allow reactants and products to be transported into and out of the interior volume; the pores provide high-area internal platforms for the metal. Common supports are amorphous metal oxides such as γ-Al_2O_3 and SiO_2. Powders of these solids consist of particles that are aggregates of small primary particles of the metal oxide held together by interparticle interactions or sometimes by binders such as vitrified clay. The pores are the spaces between the primary particles. The surfaces of metal oxide powders are highly nonuniform, exposing faces with various crystal planes and defects; the interfaces between support surfaces and metals dispersed on them are not well understood.

Not all porous materials are amorphous; some are crystalline, and these incorporate nearly uniform pores that are part of the crystal structure. Crystalline aluminosilicates (zeolites) have pores with diameters of the order of 10 Å. These materials are called molecular sieves because small molecules can pass through the pores, but molecules too large to fit are sieved out. Zeolite frameworks consist of linked TO_4 tetrahedra (T = Si, Al). Zeolites that are important supports for metal clusters include faujasites (zeolites X and Y), which have the framework structure $[Al_xSi_{192-x}O_{384}]$; a typical faujasite unit cell formula is $Na_j[(AlO_2)_j(SiO_2)_{192-j}]\cdot zH_2O$, where the Na cations are exchange ions compensating the negative charge of the framework (one per Al atom). Faujasites have three-dimensional pore structures incorporating nearly spherical cages with diameters of about 12 Å connected by apertures that are 12-membered oxygen rings, with diameters of about 7.5 Å. Zeolite LTL, which has the framework structure $[Al_xSi_{36-x}O_{72}]$, has a two-dimensional pore structure consisting of parallel, nonintersecting channels incorporating ellipsoidal cages with dimensions of about 4.8 × 12.4 × 10.7 Å; the cages are connected by 12-membered oxygen rings. The framework structure of zeolite LTL is shown in Figure 1.

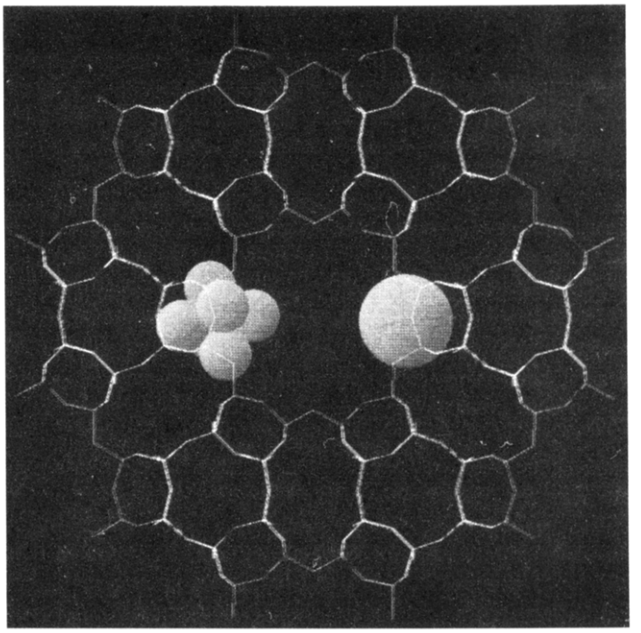

Figure 1. Computer model of zeolite LTL showing a six-atom platinum cluster. For comparison, the depiction includes a circle with a cross sectional area approximating that of a benzene molecule. Courtesy of C. L. Marshall.

Zeolite supports are important to this review because the steric restrictions offered by the cages limit the sizes of clusters that can form in them, and the restrictions of the apertures limit what can enter and leave the cages. Thus clusters can be trapped in zeolite cages. The cages are small enough to exert solvent-like effects on clusters within them, and the cages may cause the cluster structures and properties to be different from those of clusters in solution or on the more nearly planar surfaces of amorphous supports.[32] Confinement in cages may hinder cluster interactions and increase cluster stability. Because of the regularity of structure of crystalline materials, clusters in their cages may be easier to characterize structurally than clusters in amorphous materials.

Metal clusters in zeolites have been reviewed recently.[32,33]

Preparation of Supported Metal Clusters

Supported Metal Carbonyl Clusters

Metal carbonyl clusters on supports are important here because they are good precursors of supported

metal clusters, formed by decarbonylation. The routes for preparation of molecularly or ionically dispersed metal carbonyl clusters on metal oxide supports include (1) deposition from solution, (2) reaction with the support surface, and (3) syntheses from mononuclear precursors on the support surface.[18-22] The first method may not give fully dispersed surface clusters and is usually not preferred. More effective syntheses are illustrated by reactions with surface OH groups.

For example, $[Os_3(CO)_{12}]$ reacts with OH groups of SiO_2 or of γ-Al_2O_3 to give predominantly $[(\mu\text{-H})Os_3(CO)_{10}\{\mu\text{-OM}\}]$, where M = Si or Al, and the braces denote groups that terminate the bulk metal oxide.[34-36] The synthesis reaction is an oxidative addition that is analogous to solution reactions of $[Os_3(CO)_{12}]$ with alcohols. The yield is high but not precisely quantified. The chemistry[37] and bonding[38] of the surface species on silica have been discussed thoroughly. Another important class of synthesis reaction is a simple deprotonation of a hydridometal carbonyl cluster occurring on a basic metal oxide support; for example, $[H_4Os_4(CO)_{12}]$ reacts with MgO or with γ-Al_2O_3 to give the surface ion pair $[H_3Os_4(CO)_{12}^-\text{-}\{M^{n+}\}]$;[39] the cations M^{n+} are those exposed at the surface of the metal oxide support.

Surface-mediated synthesis,[22] whereby the metal carbonyl cluster is formed from a mononuclear metal carbonyl precursor (e.g., $[Rh(CO)_2(acac)]$, $[Ir(CO)_2(acac)]$, $[Pt(acac)_2]$, or $[Pt(allyl)_2]$) on the metal oxide surface, has been used to prepare numerous neutral and anionic metal carbonyl clusters. This is an efficient method for preparation of the following clusters on MgO: $[Os_5C(CO)_{14}]^{2-}$,[24] $[Os_{10}C(CO)_{24}]^{2-}$,[24] $[Rh_5(CO)_{15}]^-$,[40] and $[Pt_{15}(CO)_{30}]^{2-}$.[27] Other clusters that have been synthesized in high yields on MgO include $[HIr_4(CO)_{11}]^-$,[25] $[Ir_6(CO)_{15}]^{2-}$,[25] $[Pt_6(CO)_{12}]^{2-}$,[41] $[Pt_9(CO)_{18}]^{2-}$,[41] and $[Pt_{12}(CO)_{24}]^{2-}$.[27] $[Ir_4(CO)_{12}]$ has been prepared on γ-Al_2O_3[28] and $[H_4Os_4(CO)_{12}]$ on SiO_2.[42] Many of the yields are high, but they have not been quantified well. There are parallels between surface and solution chemistry that are predicted roughly by a comparison of surface and solvent properties.[22] For example, the syntheses on MgO take place as in basic solutions in the presence of reducing agents, and the syntheses on SiO_2 take place as in neutral solvents.

The syntheses referred to above take place in zeolite cages much as they do on surfaces of amorphous metal oxides. Syntheses in the nearly neutral NaY zeolite are similar to those occurring on γ-Al_2O_3, e.g., those of $[Ir_4(CO)_{12}]$[43] and $[Ir_6(CO)_{16}]$[44] from $[Ir(CO)_2(acac)]$. Syntheses in the more basic NaX zeolite are similar to those occurring on MgO, e.g., those of $[HIr_4(CO)_{11}]^-$ and $[Ir_6(CO)_{15}]^{2-}$.[45] Ship-in-a-bottle syntheses take place when clusters formed in zeolite cages are trapped there because they are too large to fit through the apertures.

Decarbonylation of Supported Metal Carbonyl Clusters

The preparation of supported metal clusters by decarbonylation of supported metal carbonyl clusters is exemplified by the removal of the CO ligands from the metal frame of $[Ir_4(CO)_{12}]$ dispersed on γ-Al_2O_3. The decarbonylation of the sample in helium at 200 °C, indicated by infrared and EXAFS spectroscopies, takes place with little or no disruption of the tetrahedral metal frame, as discussed below.[28] Details of the chemistry are still unknown, but the simple decarbonylation may be relatively unsurprising in view of the stability of the Ir_4 frame indicated by electrospray mass spectrometry showing that CO ligands are peeled off one by one from a salt of $[HIr_4(CO)_{11}]^-$, giving clusters represented as $HIr_4(CO)_{11-x}$ (x = 0, 1, 2, ..., 11), although whether these incorporate hydrogen is unknown.[46]

Similarly, decarbonylation of MgO-supported $[HIr_4(CO)_{11}]^-$ and of $[Ir_6(CO)_{15}]^{2-}$ takes place in helium at 300 °C.[47] Decarbonylation of MgO-supported $[Pt_{15}(CO)_{30}]^{2-}$[48] and of $[Os_{10}C(CO)_{24}]^{2-}$[49] also appears to take place without significant changes in the metal framework structures, as indicated by EXAFS spectroscopy (as discussed below).

Decarbonylation of $[Ir_4(CO)_{12}]$ and of $[Ir_6(CO)_{16}]$ in NaY zeolite cages occurs similarly,[44,50] and the decarbonylations are reversible,[50] in contrast to decarbonylations of the same clusters on MgO.[51] Infrared spectra show that $[Ir_4(CO)_{12}]$ (or $[Ir_6(CO)_{16}]$) was decarbonylated by treatment in H_2 at 300 °C.[50] When CO was adsorbed on the decarbonylated clusters at −196 °C and the temperature raised with the sample in CO, mononuclear iridium carbonyls formed at about −30 °C. These were converted at about 50 °C into $[Ir_4(CO)_{12}]$ and at about 125 °C into $[Ir_6(CO)_{16}]$.[50]

Formation of Metal Clusters in Zeolite Cages by Reduction of Exchange Cations

Zeolite-supported metal clusters have most commonly been prepared by ion exchange followed by reduction.[52-54] Usually the metals are introduced as cationic complexes, (e.g., $[Pt(NH_3)_4]^{2+}$), which replace cations such as Na^+ in the zeolite and are then decomposed by heating in O_2 or air (calcination) and reduced in H_2. The metal complex may be introduced instead by impregnation with an aqueous solution, typically by the incipient wetness method, whereby just enough solution is added to fill the pores of the solid. Sample preparation is not easily reproduced, depending, for example, on the nature and loading (and thus crystallographic location) of the cations, the presence of oxidizing agents such as hydroxyl groups, and the presence of residual water during the treatments. Because samples prepared in this way are typically nonuniform in structure, only little is written in this section. The synthesis methods work for zeolites, but they may often give larger clusters and/or particles of metal when amorphous supports are used. Reduction of metals in zeolites often leads to metal clusters or particles that are too large to fit in the cages, and it may then be accompanied by the breakup of the zeolite framework and/or migration of the metal outside of the intracrystalline space.

Cations of noble metals in zeolites are easily reduced by H_2, but proper activation and reduction treatments that give the highest metal dispersions are not easily predicted. Appropriate treatments of ion-exchanged zeolites are needed to minimize migration and sintering of the metal. For example, prior to reduction in H_2, it is usually necessary to eliminate NH_3 produced by thermal decomposition of NH_4^+ ions or ammine complexes, because reduction

of metal ions in the presence of evolving NH_3 leads to formation of agglomerated metal. Direct reduction of noble metal cations by H_2 at high temperatures may lead to formation of neutral metal hydrides, which are mobile, causing metal agglomeration and low metal dispersions.[55] Water is also detrimental to metal dispersion.[55]

Activation in flowing O_2 prior to reduction in H_2 gives highly dispersed platinum clusters in zeolites. The temperature of O_2 treatment has a critical influence on metal dispersion. For example, Dalla Betta and Boudart,[55] investigating a sample prepared from $Pt(NH_3)_4Cl_2$ in CaY zeolite, found that calcination in O_2 at 350 °C followed by treatment in H_2 at 400 °C gave highly dispersed platinum in the zeolite. Reagan et al.[56] found that ammonia from the platinum complex reduced the platinum, concluding that reduced platinum is always the product of the thermal decomposition (at 300 °C or higher temperatures) of platinum ammines in Y zeolite, even in air. These authors recommended 300 °C as the optimum calcination temperature in air, and their result was reinforced by Chester.[57] Similarly, highly dispersed platinum (with about six atoms per cluster, on average) in H-mordenite was prepared from $Pt(NH_3)_4(OH)_2$, with calcination at 350 °C and reduction in H_2 at 350 °C.[58] Platinum clusters were formed in KLTL zeolite by aqueous impregnation with tetraammineplatinum(II) nitrate followed by calcination at 260 °C and reduction in H_2 at 500 °C.[59] The patent literature[60] also refers to this low calcination temperature, which is inferred to favor the formation of extremely small clusters in zeolite L.

Alternatively, reduction of noble metals in zeolite LTL has been reported to give extremely small noble metal clusters even when the calcination step is omitted. Vaarkamp et al.[61] prepared platinum clusters of about five or six atoms each, on average, from $Pt(NH_3)_4(NO_3)_2$ in zeolite BaKLTL by reduction at 500 °C in the absence of calcination. A computer model of 6-atom clusters in LTL zeolite is shown in Figure 1. Triantafillou et al.[62] similarly prepared iridium clusters from $[Ir(NH_3)_5Cl]Cl_2$ in zeolite KLTL by reduction in H_2 at 300 or 500 °C, without calcination; the average cluster contained about 5–6 iridium atoms.

Deposition of Size-Selected Gas-Phase Metal Clusters

Beams of gas-phase metal clusters generated by bombardment of metallic targets can be size selected by a mass spectrometer. When fractionated beams of these clusters with low kinetic energies impinge on planar surfaces in an ultrahigh vacuum chamber, the clusters are deposited in a dispersed, size-selected form. The few such samples are those mentioned above, Pt_n, where $n = 1-6$, on oxidized silicon wafers (SiO_2) and on carbon films,[30] and Pt_n and Pd_n, where $n = 1-15$, on Ag(110) single crystals.[31]

Structural Characterization of Supported Metal Clusters

The practical way to apply metal clusters as catalysts is to use them dispersed on supports. These materials pose a challenge in characterization science because the clusters are small, usually nonuniform, and present in only low loadings in solids. Only recently have the most incisive physical methods for identification of such small dispersed clusters become available, including, for example, EXAFS spectroscopy, high-resolution electron microscopy, ^{129}Xe NMR spectroscopy, scanning tunneling microscopy, and atomic force microscopy. These methods, complemented by others, including H_2 and CO chemisorption and wide-angle X-ray scattering, have opened the way to investigation of the synthesis and catalytic properties of supported metal clusters.

Imaging Methods

Transmission electron microscopy is valuable because it allows imaging of even the smallest supported clusters of a heavy metal such as platinum. However, most of the samples are air sensitive, and few instruments are available for high-resolution microscopy in the absence of air. Dark field microscopy has been used to advantage for platinum clusters consisting of < 20 atoms each in zeolite KLTL.[63] Even single platinum atoms can be detected on zeolite supports thinner than about 200 Å, but the precision with which clusters can be pinpointed in the structure is limited by beam damage-induced distortion of the zeolite framework.[63] Other imaging techniques, including scanning tunneling microscopy and atomic force microscopy, are potentially of value for clusters on planar supports, but well-defined supported metal clusters in this form have not yet been investigated by the technique.

Chemisorption

Hydrogen chemisorption is not yet a routine characterization method for supported metal clusters because stoichiometries of chemisorption on the clusters are not well known and are different from those of chemisorption on metal crystallites.[51] Supported iridium clusters chemisorb several times less hydrogen per exposed atom than supported iridium particles,[51] and these adsorb even less than transition metal clusters in the gas phase.[64] Temperature-programmed desorption of chemisorbed hydrogen from supported iridium clusters indicates that some hydrogen is much more tightly bound than hydrogen on metallic iridium particles. Chemisorption of CO is also of limited value because CO typically reacts with supported clusters, leading to changes in cluster structure.

Work is needed to characterize the reactivities of supported metal clusters with probe molecules and to establish methods for counting exposed metal sites.

EXAFS Spectroscopy

EXAFS spectroscopy,[65] although it is still immature and developing rapidly, provides structure data characterizing supported clusters, most precisely when they are very small and nearly uniform.[66] The technique is limited because it provides only average structural information and relatively imprecise values of coordination numbers. Furthermore, the best data are obtained at very low temperatures (e.g., liquid nitrogen temperature).

Table 2. Supported Iridium Clusters Formed by Decarbonylation of Supported Iridium Carbonyl Clusters: Characterization by EXAFS Spectroscopy[a]

support (dehydroxylation temp, °C)	decarbonylation temp, °C, and gas	precursor	cluster modeled as	N	R, Å	$\Delta\sigma^2$, Å^2	ΔE_0, eV	ref
γ-Al_2O_3 (120)	300, He	$[Ir_4(CO)_{12}]$	Ir_4 tetrahedra	2.9	2.69	0.0031	0.83	28
MgO (400)	300, He; 300, H_2	$[HIr_4(CO)_{11}]^-$	Ir_4 tetrahedra	3.1	2.69	0.0011	1.22	67
MgO (400)	300, He; 300, H_2	$[HIr_4(CO)_{11}]^-$	Ir_4 tetrahedra	3.1	2.70	0.0023	0.50	68
MgO (700)	325, He; 300, H_2	$[HIr_4(CO)_{11}]^-$	Ir_4 tetrahedra	3.0	2.69	0.0048	3.9	69
NaY zeolite (500)	325, He; 325, H_2	$[Ir_4(CO)_{12}]$ formed from $[Ir(CO)_2(acac)]$	Ir_4 tetrahedra	3.4	2.70	0.0030	0.06	43
NaX zeolite (500)	300, H_2	$[HIr_4(CO)_{11}]^-$ formed from $[Ir(CO)_2(acac)]$	Ir_4 tetrahedra	3.0	2.71	0.0029	2.77	45
MgO (400)	300, He; 300 H_2	$[Ir_4(CO)_{12}]$	Ir_4, mixture of tetrahedra and rafts	2.6	2.71	0.0006	−5.2	47

[a] Notes: N is coordination number; R, the average absorber-backscatterer distance; $\Delta\sigma^2$, the Debye−Waller factor; and ΔE_0, the inner potential correction. Typical experimental errors in N and R are approximately ±20% and ±2%, respectively.

Table 3. Supported Metal Clusters Formed by Decarbonylation of Supported Metal Carbonyl Cluster Precursors and Characterized by EXAFS Spectroscopy[a]

support (pretreatment temp, °C)	precursor	cluster modeled as	metal−metal first-shell coordination number	metal−metal distance, Å	$\Delta\sigma^2$, Å^2	ΔE_0, eV	comment	ref
MgO (400)	$[Ru_3(CO)_{12}]$	Ru_3	1.7	2.64	not stated	not stated	Ru−O contributions indicate bonding to support	70
γ-Al_2O_3 (300)	$[Ru_3(CO)_{12}]$	Ru_6	3.1	2.64	not stated	not stated	data not sufficient to determine cluster nuclearity; raft structure suggested	70
γ-Al_2O_3 (500)	$[H_3Re_3(CO)_{12}]$	Re_3	2.0	2.67	0.00086	−3.04	cationic raft structure suggested on basis of short Re−Re distance and evidence of Re−O bonding	71
zeolite 5A, Ca form	$Pd(NH_3)_4(NO_3)_2$	Pd_6?	3.5	not stated	not stated	not stated	structure not stated by authors; data suggestive of Pd_6	72
MgO (400)	$[Ir_6(CO)_{16}]$ formed from $[Ir(CO)_2(acac)]$	Ir_6 in mixture with Ir rafts	2.7	2.72	0.004	−4.5	data indicate mixture of surface structures	47
NaY zeolite (25)	$[Ir_6(CO)_{16}]$ formed from $[Ir(CO)_2(acac)]$	Ir_6	3.6	2.71	0.0035	−2.00	data consistent with Ir_6 octahedra	44
MgO (400)	$[Pt_{15}(CO)_{30}]^{2-}$ formed from Na_2PtCl_6	Pt_{15}	3.7	2.76	0.0033	−0.87	data not sufficient to determine cluster nuclearity	48
MgO (400)	H_2OsCl_6	Os_{10}	3.8	2.67	0.00037	1.2	data not sufficient to determine cluster nuclearity	73

[a] Notation as in Table 2.

The science of metal clusters on supports was almost without a structural foundation before EXAFS spectroscopy provided it. EXAFS results have been reported for a number of supported clusters derived from metal carbonyl clusters on metal oxide supports (Tables 2 and 3). The most thoroughly investigated of these are clusters formed from tetrairidium carbonyls (Table 2). For example, supported clusters formed by decarbonylation of γ-Al_2O_3-supported $[Ir_4(CO)_{12}]$, which has a tetrahedral metal frame, have an average Ir−Ir first-shell coordination number of about 3, the value for a tetrahedron (Table 2). However, the experimental error in this coordination number is about ±20%, and there is no confirming structural information and no technique that easily provides it, although EXAFS data may provide additional evidence of structure, as summarized by van Zon et al.[47] With this caveat, the structures are modeled as Ir_4 tetrahedra, except as noted in Table 2.

Confirming evidence of the ability of EXAFS spectroscopy to determine the metal−metal coordination numbers was obtained for a family of iridium carbonyl clusters (precursors of the supported iridium clusters) that were characterized both by EXAFS spectroscopy and by complementary physical methods, including infrared spectroscopy in the ν_{CO} region and extraction of the anionic clusters into solution and identification by infrared spectroscopy and mass spectrometry (Table 4).

For example, the tetrahedral metal frame has been demonstrated by X-ray diffraction crystallography for $[Ir_4(CO)_{12}]$.[76] EXAFS spectra of solid $[Ir_4(CO)_{12}]$ are in agreement with the crystallographic data, showing a first-shell Ir−Ir coordination number of 3 (and no higher-shell Ir−Ir contributions) (Table 4). This

Table 4. Summary of EXAFS Results Characterizing Supported and Unsupported Iridium Carbonyl Clusters[a]

Ir cluster/support	Ir−Ir coordination number	Ir−Ir bond distance, Å	$\Delta\sigma^2$, Å^2	ΔE_0, eV	ref
$[Ir_4(CO)_{12}]$ mixed with boron nitride	3.0[b]	2.69[c]	−0.0008	−0.77	74
$[Ir_4(CO)_{12}]$/NaY zeolite	2.6[b]	2.68[c]	0.0004	4.88	43
$[HIr_4(CO)_{11}]^-$/MgO	3.2[d]	2.71[e]	0.002	3.81	67
$[Ir_6(CO)_{15}]^{2-}$/MgO	4.1[f]	2.77[g]	0.0010	not stated	75

[a] Notation as in Table 2. [b] Crystallographic value 3 (from ref 76). [c] Crystallographic value 2.69 Å (from ref 76). [d] Crystallographic value 3 (from ref 77). [e] Crystallographic value 2.73 Å (from ref 77). [f] Crystallographic value 4 (from ref 78). [g] Crystallographic value 2.77 Å (from ref 78).

same value of the coordination number (within experimental error) has also been confirmed by EXAFS spectroscopy for $[HIr_4(CO)_{11}]^-$ on the surface of MgO (Table 4), and crystallographic data confirm the tetrahedral metal frame in this cluster in the solid state.[77] The presence of this cluster anion on the surface of MgO was confirmed by infrared spectroscopy and by extraction into solution by ion exchange, although the purity of the cluster on the surface was less than 100%.[67] Decarbonylated iridium clusters with Ir−Ir coordination numbers of nearly 3 have also been prepared on various metal oxide supports (Table 2).

Thus within the limits of accuracy of the EXAFS technique, the data show that a whole family of tetrahedral Ir_4 clusters has been prepared on solid supports. These are the simplest and best-defined supported metal clusters reported, and they provide an unprecedented opportunity to determine the catalytic properties of nearly unique metal clusters on supports.

The structures of the supported metal clusters depend on the preparation conditions and are affected by traces of O_2 impurities. For example, structurally nonuniform iridium clusters were obtained from $[HIr_4(CO)_{11}]^-$ on a MgO surface that was partially dehydroxylated by treatment at 400 °C.[47] The decarbonylated clusters were evidently not simply Ir_4 tetrahedra, as would have resulted if the metal frame of the precursor had remained unchanged during the decarbonylation. The simplest model that represents the EXAFS data well is a mixture of about 50% tetrahedra and 50% rafts.[47] Later preparations, perhaps with better air exclusion and with other MgO pretreatment temperatures, gave samples that were characterized by EXAFS data modeled well as Ir_4 tetrahedra (Table 2), on γ-Al_2O_3, MgO, and NaY zeolite (Table 2). When the synthesis was attempted on hydroxylated MgO, clusters larger than Ir_4 were observed.[69]

Supported iridium clusters with relatively simple structures have also been prepared from $[Ir_6(CO)_{15}]^{2-}$ on MgO.[47] Decarbonylation of these cluster anions on MgO gave a sample that was modeled as a mixture of Ir_6 octahedra and rafts. In the apparently more stabilizing environment of NaY zeolite supercages, clusters were formed by decarbonylation of $[Ir_6(CO)_{16}]$ that may be predominantly octahedra of Ir_6.[44] However, even fully analyzed, high-quality EXAFS data are not sufficient for an unequivocal structure determination of a cluster as large as a six-atom cluster. The Ir−Ir first-shell coordination number of about 4 is consistent with the presence of Ir_6 octahedra, but the data were not sensitive enough to determine whether there was a higher shell Ir neighbor (as would be expected at the opposite apex of an octahedron). EXAFS results obtained for MgO-supported $[Ir_6(CO)_{15}]^{2-}$ are consistent with the presence of clusters with an octahedral metal frame (Table 4), and the presence of this anion was confirmed by infrared spectra and by the exact agreement of the Ir−Ir first-shell distance determined by EXAFS spectroscopy of the supported cluster anion and that determined crystallographically for the anion in a salt (Table 4). Thus, there are data that are consistent with the inference that Ir_6 octahedra were formed on the surface of MgO, but the structural model for the decarbonylated clusters is less firm than that mentioned above for the tetrairidium clusters.

A summary of zeolite-supported metal clusters prepared from metal salts (without the involvement of metal carbonyl clusters) is given in Table 5. Included here are only samples that have been characterized by EXAFS spectroscopy and incorporate extremely small clusters. The extensive literature of zeolite-supported metals characterized only by other methods is reviewed elsewhere.[32,33,52-54,81] The synthetic methods used to prepare metal clusters in zeolites are similar to those used for most conventional supported metal catalysts. The zeolites appear to be different from amorphous supports in giving such highly dispersed and nearly uniform metal clusters; the cages and apertures are inferred to limit the sizes of the clusters by hindering the migration of species that migrate and sinter readily on amorphous supports. Nonetheless, it must be assumed that the samples listed in Table 5 have distributions of cluster sizes, although the available methods do not provide good evidence of the distributions. It seems likely that zeolite-supported metal clusters made from metal carbonyl clusters (Tables 2 and 3) incorporate more nearly uniform clusters than the samples made by conventional methods from metal salts, but this suggestion is not yet tested.

It has long been recognized that very highly dispersed metals in zeolites can be prepared; early authors even postulated atomic dispersions of zerovalent noble metals,[82] and this idea is still advocated.[83] However, entirely convincing evidence of atomically dispersed metals (other than exchange ions) is still lacking. The literature of zeolite-supported metals, e.g., that cited by Samant and Boudart,[81] indicates the difficulty of characterizing supported metal clusters and the advances resulting from the use of EXAFS spectroscopy. A succession of experiments characterizing platinum in zeolite Y with essentially all the available techniques, reviewed elsewhere,[81] has led to estimates of platinum nuclearities ranging from 6 to about 40.

Table 5. Zeolite-Supported Metal Clusters Formed from Salt Precursors[a]

support	precursor	characterization methods	metal–metal coordination number	approximate average cluster nuclearity	comment	ref
BaKLTL zeolite	$Pt(NH_3)_4(NO_3)_2$	EXAFS, TEM, H_2 chemisorption	3.7	5–6	sample not calcined after addition of Pt; reduced at 500 °C	61
KLTL zeolite	$Pt(NH_3)_4(NO_3)_2$	EXAFS, H_2 chemisorption, TPD of hydrogen	4.0 ± 0.1	6	sample not calcined after addition of Pt; reduced at 300 °C	79, 80
KLTL zeolite	$Pt(NH_3)_4(NO_3)_2$	EXAFS, H_2 chemisorption, TPD of hydrogen	4.8 ± 0.2	10	sample not calcined after addition of Pt; reduced at 500 °C	79, 80
KLTL zeolite	$Pt(NH_3)_4(NO_3)_2$	EXAFS, H_2 chemisorption, TPD of hydrogen	4.9 ± 0.1	12	sample not calcined after addition of Pt; reduced at 600 °C	79, 80
HLTL zeolite	$Pt(NH_3)_4(NO_3)_2$	EXAFS, H_2 chemisorption, TPD of hydrogen	4.1 ± 0.1	6	sample not calcined after addition of Pt; reduced at 300 °C	79, 80
HLTL zeolite	$Pt(NH_3)_4(NO_3)_2$	EXAFS, H_2 chemisorption, TPD of hydrogen	4.4 ± 0.1	9	sample not calcined after addition of Pt; reduced at 500 °C	79, 80
HMAZ zeolite	$Pt(NH_3)_4(NO_3)_2$	EXAFS, H_2 chemisorption	2.9 ± 0.2	4	sample not calcined after addition of Pt; reduced at 500 °C	79
HMOR zeolite	$Pt(NH_3)_4(OH)_2$	EXAFS, TPD of hydrogen	3.7	6	sample calcined at 350 °C after addition of Pt; reduced at 350 °C	58
KHMOR zeolite	$Pt(NH_3)_4(OH)_2$	EXAFS, TPD of hydrogen	3.9	6	sample calcined at 350 °C after addition of Pt; reduced at 350 °C	58

Photoelectron Spectroscopy

Size-selected platinum and palladium clusters on planar supports have been investigated with X-ray and ultraviolet photoemission spectroscopy.[30,31] Each of the species Pt_n (n = 1, 2, ..., 6) on SiO_2[30] has a distinct spectrum, different from that of metallic platinum. Structural data for the supported clusters are still lacking. Results characterizing Pt_n (n = 1, 2, ..., 15) on Ag(110) similarly indicate distinct core level binding energies for the different species, but the line width was found to increase and then level off for clusters containing more than six platinum atoms.[31] Calculations suggested chain structures for the smaller clusters on Ag(110).

Open Questions

Rapid progress in the characterization of supported metal clusters has taken place in the preceding few years, with the opportunities presented by the successes in synthetic chemistry, which themselves benefited from the characterization methods. However, much remains to be learned. The structures and reactivities of supported metal clusters are still not known well. The effects of supports on cluster structure and the nature of the cluster–support interface are less than well understood.[47] Powder metal oxide supports are structurally nonuniform, and it has been postulated that clusters reside preferentially at defect sites;[84] experiments with structurally well defined metal clusters on planar or single-crystal metal oxides are needed to determine how the support structure affects cluster structure and properties. Reported assessments of electronic properties of supported clusters are still not consistent with each other. Theoretical chemistry is beginning to have an impact on the assessment of electronic properties, with calculations having been reported for Ir_4 and Ir_{10},[85] but it is still too early for theories to account reliably for the influence of the support.

Summary

Supported metal clusters have now been prepared that are nearly uniform (nearly molecular), although work is needed to determine structures and properties with greater precision. These samples offer a long-awaited opportunity to determine the catalytic properties of metal clusters. It is now feasible to design experiments to determine the separate influences of cluster size, electronic effects, and metal–support effects on catalyst performance. Results of the first such experiments are summarized below.

Catalysis by Supported Metal Clusters

It is likely that metal clusters have been present for years in conventional supported metal catalysts, such as those used for naphtha reforming, but because of the difficulty of distinguishing the small clusters from larger metal crystallites, it has not been possible to identify and define the roles of clusters. Rather, evidence of catalysis by supported metal clusters has arisen only recently, made possible by syntheses that give catalysts containing metal almost exclusively in the form of clusters. The following section is a summary of catalytic results for supported metal clusters that have been characterized both before and after catalysis by EXAFS spectroscopy, with the data demonstrating the lack of significant changes in the cluster nuclearities as a result of catalysis.

Catalysis by Supported Ir_4 and Ir_6 Clusters

Catalytic properties of supported clusters identified as primarily Ir_4 or Ir_6 were reported by Xu et al.,[46]

Table 6. EXAFS Results Characterizing Fresh and Used Supported Metal Cluster Catalysts

sample number	catalyst precursor	support	treatment/catalysis[a]	fresh catlayst		used catalyst		ref
				N[b]	R,[c] Å	N[b]	R,[c] Å	
1	$[HIr_4(CO)_{11}]^-$	MgO	none	3.2	2.71			46, 67, 75
2	$[Ir_4(CO)_{12}]$	γ-Al_2O_3	decarbonylation and catalysis of toluene hydrogenation	2.9	2.69	3.2	2.68	28, 46
3	$[HIr_4(CO)_{11}]^-$	MgO	decarbonylation and catalysis of toluene hydrogenation	3.2	2.71	2.8	2.69	46, 67, 75
4	$[Ir_6(CO)_{16}]$	NaY zeolite	decarbonylation and catalysis of toluene hydrogenation			3.9	2.70	46
5	$[Ir_6(CO)_{15}]^{2-}$	MgO	decarbonylation and catalysis of toluene hydrogenation			4.1	2.69	46
6	$[HIr_4(CO)_{11}]^-$	MgO	decarbonylation, treatment in H_2 at 300 °C, and catalysis of toluene hydrogenation	3.1	2.70	3.1	2.70	46
7	$[Ir_6(CO)_{15}]^{2-}$	MgO	decarbonylation, treatment in H_2 at 300 °C, and catalysis of toluene hydrogenation	3.8	2.69	3.7	2.70	46
8	$[Ir_4(CO)_{12}]$	γ-Al_2O_3	decarbonylation, treatment in H_2 at 300 °C, and catalysis of toluene hydrogenation			5.4	2.67	46
9	$[Ir_6(CO)_{16}]$	NaY zeolite	decarbonylation, treatment in H_2 at 300 °C, and catalysis of toluene hydrogenation	3.6	2.71	4.1	2.69	44, 46
10	$[HIr_4(CO)_{11}]^-$	MgO	decarbonylation, treatment in H_2 at 300 °C, and catalysis of cyclohexene hydrogenation			3.3	2.71	46
11	$[HIr_4(CO)_{11}]^-$	MgO	decarbonylation, treatment in H_2 at 300 °C, and catalysis of propane hydrogenolysis	3.35 ± 0.15	2.730 ± 0.005	3.26 ± 0.23	2.735 ± 0.006	68
12	$[Os_{10}C(CO)_{24}]^{2-}$	MgO	decarbonylation, treatment in H_2 at 300 °C, and catalysis of n-butane hydrogenolysis	4.7	2.67	5.0	2.68	49, 73
13	$Pt(NH_3)_4(OH)_2$	HMOR zeolite	calcination at 350 °C, treatment in H_2 at 350 °C, and catalysis of n-hexane isomerization	3.7	2.72	not stated, but nearly 3.7	not stated	58

[a] Conditions of catalysis experiments stated in Table 7. [b,c] N is the first-shell metal−metal coordination number, and R is the metal−metal distance; both determined by EXAFS spectroscopy.

who investigated classic structure-insensitive reactions, namely, cyclohexene hydrogenation and toluene hydrogenation. EXAFS spectroscopy showed that the first-shell Ir−Ir coordination numbers characterizing both the fresh and used MgO-supported catalysts made by decarbonylation of supported $[Ir_4(CO)_{12}]$ or $[HIr_4(CO)_{11}]^-$ are indistinguishable from 3, the value for a tetrahedron, as in $[Ir_4(CO)_{12}]$ and $[HIr_4(CO)_{11}]^-$ (Table 6). The decarbonylated clusters retained this metal frame. EXAFS data show that the decarbonylated Ir_6 clusters had metal frames indistinguishable from the octahedra of the precursor hexairidium carbonyls, indicated by the coordination number of approximately 4 (Table 6).

Catalytic activities of these clusters (Table 7) are reported as turnover frequencies; these are rates per total iridium atom for such small clusters. Rates were also reported for conventional (structurally nonuniform) supported catalysts consisting of aggregates of metallic iridium on supports; these rates are reported per surface iridium atom, determined by H_2 chemisorption. The decarbonylated iridium clusters are markedly less active than the iridium particles on MgO (Table 7). The clusters represented as Ir_6 are several times less active than those represented as Ir_4. Changing the support from MgO to γ-Al_2O_3 to zeolite NaY had little effect on the activities of the decarbonylated clusters (Table 7). The orders of reaction in toluene and in H_2 were found to be approximately 0 and 1, respectively, for the supported iridium cluster catalysts as well as for supported iridium particles.

Pretreatment in H_2 at 300 °C did not lead to a significant change in the metal framework structures of MgO-supported Ir_4 and Ir_6, as shown by EXAFS, but it did lead to a decrease in their activities for toluene hydrogenation (Table 7). The results suggest that hydrogen bonded strongly to the clusters and inhibited catalysis. However, the effect of hydrogen illustrated by these data is not the same as that observed for Ir_6 in NaY zeolite. The hydrogen pretreatment led to a doubling of the activity of this catalyst without a substantial change in the metal framework structure. The data suggest that the different supports lead to different effects of hydrogen treatment, but the issues are unresolved.

Additional evidence of support effects is shown by the data for Ir_4 supported on γ-Al_2O_3; following treatment in H_2 at 300 °C, the catalytic activity (per total Ir atom) increased 10-fold (Table 7). This increase is explained, at least in part, by the EXAFS result for the used catalyst, which shows that the

Table 7. Catalytic Activities of Supported Metal Clusters and Supported Metallic Particles

sample number[a]	catalyst modeled as	support	catalytic reaction[b]	H_2 treatment temperature of catalyst, °C	$10^3 \times$ TOF,[c] s^{-1}	ref
1	$[HIr_4(CO)_{11}]^-$	MgO	toluene hydrogenation	no treatment	0.00	46
2	Ir_4	γ-Al_2O_3	toluene hydrogenation	no H_2 treatment	0.94	46
3	Ir_4	MgO	toluene hydrogenation	no H_2 treatment	0.63	46
4	Ir_6	NaY zeolite	toluene hydrogenation	no H_2 treatment	0.25	46
5	Ir_6	MgO	toluene hydrogenation	no H_2 treatment	0.23	46
6	Ir_4	MgO	toluene hydrogenation	300	0.17	46
7	Ir_6	MgO	toluene hydrogenation	300	0.03	46
8	aggregates of about 20 atoms each, on average, formed from Ir_4	γ-Al_2O_3	toluene hydrogenation	300	9.9[d]	46
9	Ir_6	NaY zeolite	toluene hydrogenation	300	0.52	46
10	Ir_4	MgO	cyclohexene hydrogenation	300	18	46
11	Ir_4	MgO	propane hydrogenolysis	300	20	68
12	approximately Os_{10}	MgO	*n*-butane hydrogenolysis	300		73
13	approximately Pt_6, on average	HMOR zeolite	*n*-hexane isomerization	350	not stated; rate influenced by diffusion	58
14	Ir crystallites	MgO	toluene hydrogenation	500	2.0	46

[a] Sample numbers match those of Table 6. [b] Reaction conditions: Each reaction except cyclohexene hydrogenation carried out with vapor-phase reactants in a once-through plug flow reactor operated at atmospheric pressure. Cyclohexene hydrogenation carried out with liquid-phase cyclohexene in *n*-hexane solvent saturated with H_2 flowing through the stirred reactor, which was held at atmospheric pressure. [c] TOF for toluene hydrogenation at 60 °C; for cyclohexene hydrogenation at 25 °C; for propane hydrogenolysis at 200 °C with a H_2/hydrocarbon molar ratio of 2.5; for *n*-butane hydrogenolysis at 227 °C with a *n*-butane/H_2/He molar ratio of 1/10/9. [d] In contrast to the activities of the other catalysts, the activity of this catalyst is expressed per total Ir atom to facilitate the comparison with the results for sample 2. The comparison shows that the activity, even per total Ir atom, increased as a result of aggregation of the Ir caused by pretreatment of the sample in hydrogen.

iridium had aggregated to give clusters of about 20 atoms each, on average (Table 6). The data show that the support significantly affects the stability of the clusters, whereas it hardly affects their intrinsic catalytic activity. The data are consistent with the suggestion that NaY zeolite helps to stabilize the clusters.

Although the Ir_4 and Ir_6 clusters catalyze the same reactions as metallic iridium particles, their catalytic character is different, even for structure-insensitive hydrogenation reactions. It is inferred[46] that the clusters are metallike but not metallic; we refer to them as quasi molecular. Thus these data show the limit of the concept of structure insensitivity; it pertains to catalysis by surfaces of structures that are metallic, i.e., present in three-dimensional particles about 10 Å in diameter or larger.

If the supported metal clusters are to be regarded as quasi molecular, it follows that the support provides part of a ligand shell, which presumably affects the catalytic activity, much as ligands affect the catalytic activities of molecular metal clusters. The suggestions that some supported metal clusters have a cationic character and are chemically bonded to the supports (Table 3) is consistent with the role of the metal oxide support as a multidentate ligand. The lack of a significant effect of changing the support on the catalytic activities indicated in Table 7 is suggested to be a consequence of the fact that the supports are all metal oxides that are not much different from each other as ligands.

MgO-supported clusters formed by decarbonylation of $[HIr_4(CO)_{11}]^-$ were also investigated as catalysts for a structure-sensitive reaction, propane hydrogenolysis.[68] The decarbonylated cluster had an average Ir−Ir coordination number of 3.1, consistent with the hypothesis that the tetrahedral metal frame was largely retained after decarbonylation. The used catalyst was characterized by an Ir−Ir coordination number of 3.2. The lack of any significant change in the average cluster size indicates the stability of the supported catalyst, which is modeled as tetrairidium clusters. The catalyst performance data confirm the stability, indicated by a lack of change in the activity in a flow reactor, following a break-in period. The turnover frequency (Table 7) was found to be 2 orders of magnitude less than that of a conventionally prepared MgO-supported iridium catalyst consisting of variously sized iridium crystallites, shown by transmission electron microscopy to be about 30 Å in average diameter. These data are consistent with the identification of propane hydrogenolysis as a structure-sensitive reaction, but a reservation must be expressed about this inference: Because the supported crystallites are so much more active than the supported clusters, it is difficult to rule out the possibility that a small fraction of the clusters had aggregated on the support surface to give larger species and that these provided the surfaces for the observed catalytic activity. Data for *n*-butane hydrogenolysis by MgO-supported clusters formed by decarbonylation of $[Os_{10}C(CO)_{24}]^{2-}$ and modeled as Os_{10} are also consistent with the structure sensitivity of hydrogenolysis.[49,73]

Catalysis by Clusters of Pt and of Ir in Zeolite LTL

Supported metal clusters as small as those described in the preceding paragraphs are important in catalytic technology. These catalysts are now used commercially for naphtha reforming for production of aromatics.[86,87] They consist of platinum clusters in zeolite LTL made basic by the presence of K^+ or K^+ and Ba^{2+} exchange ions.[88−90]

Several industrially prepared catalysts of this type had almost all the clusters in the zeolite pores, as

shown by EXAFS spectroscopy and other methods (Table 5); for example, EXAFS spectra indicate first-shell Pt−Pt coordination numbers of 4−5, indicating clusters of, on average, about 5−12 atoms. Dark field electron microscopy results[63] mentioned above have led to a similar conclusion for industrially prepared catalysts.

The catalyst performance is illustrated by data of Lane et al.[59] for conversion of *n*-hexane in the presence of excess H_2 at 330−440 °C and atmospheric pressure. Primary products result from both 1,6 and 1,5 ring closure, giving benzene and methylcyclohexane, respectively. The catalyst is remarkable for its benzene selectivity, which increases with increasing conversion of *n*-hexane because some of the primary products are further converted into benzene.

Several explanations have been advanced for the unique performance of Pt/LTL zeolite catalysts. There is general agreement that dehydrocyclization is catalyzed by the platinum clusters alone, with the support providing no catalytic sites.[59,86,91] The support must be nonacidic to prevent yield loss by acid-catalyzed isomerization and hydrocracking.[86,92] The more basic is the LTL zeolite support, the higher is the aromatic selectivity. The interaction of the platinum clusters with the basic support has been suggested to result in an increase in the electron density on platinum that favors the catalysis.[93−96] The steric environment of the platinum clusters may also be important; the one-dimensional pore structure of the LTL zeolite has been suggested to orient the straight-chain paraffin parallel to the pore axis, thereby increasing the probability of terminal adsorption.[97] Because well-prepared catalysts incorporate extremely small clusters, with almost no platinum outside the pores, the high selectivity is associated with the low hydrogenolysis activity of platinum clusters smaller than about 10 Å.[92] The small zeolite cavities favor small, stable entrapped clusters.

Iridium clusters in zeolite KLTL, consisting of four to six atoms on average, have also been prepared, by reduction of $[Ir(NH_3)_5Cl]Cl_2$ in H_2 at temperatures >300 °C.[62] Notwithstanding the small cluster size, the basic support environment, and the location in the LTL zeolite pore structure, the clusters were found to be similar to other iridium catalysts for conversion of *n*-hexane and H_2, having a poor selectivity for aromatization and a high selectivity for hydrogenolysis. Thus the iridium clusters are much less selective than platinum clusters of nearly the same size in the zeolite. The comparison is consistent with the inference that selective naphtha aromatization catalysts require both a nonacidic support and a metal with a low hydrogenolysis activity, like platinum.

In summary, although the catalysis is complex and not yet fully understood, it is evident that maximization of aromatization selectivity results from the choice of a catalytic metal with a low intrinsic activity for hydrogenolysis (platinum) and optimization of the support alkalinity and steric environment, which favors small clusters (which are highly selective) and perhaps otherwise favors the desired ring closure.

Assessment and Opportunities

Supported metal clusters are a new class of catalyst made possible by syntheses involving organometallic chemistry on surfaces, gas-phase cluster chemistry, and novel preparations in zeolite cages. The synthetic chemistry would not have been possible without the guidance of new characterization science; EXAFS spectroscopy is the technique that has provided the most insight into structures of supported metal clusters. Clusters such as Ir_4, Ir_6, and Pt_n (where *n* is about 6) are small enough to be considered quasi molecular rather than metallic. Their catalytic properties are distinct from those of metallic particles, even for structure-insensitive reactions.

The MgO-supported Ir_4 and Ir_6 clusters are stable catalysts, as shown both by EXAFS results indicating retention of the metal framework structures during catalysis (Table 6) and by the lack of significant changes in the catalytic activities during steady-state operation in flow reactors.[46,68] Thus supported metal cluster catalysts seem to be robust enough for practical application, although questions about their possible regeneration remain to be answered. The size dependence of the catalytic properties of the supported clusters is consistent with the observations of unique reactivities of size-selected gas-phase metal clusters.

The results suggest that it may be fruitful to search for reactions for which supported metal clusters have catalytic properties superior to those of conventional supported metals. The catalytic activities of clusters modeled as Ir_4 and Ir_6 are less than those of supported iridium particles, at least for hydrocarbon hydrogenation and hydrogenolysis reactions, but the important opportunity in catalysis may be to find reactions for which the activity or selectivity of supported metal clusters is superior to those of conventional supported metals. The high selectivity of Pt/LTL zeolite catalysts for alkane dehydrocyclization, which is now exploited commercially, appears to be the most persuasive indication of the value of supported metal cluster catalysts. The high selectivity of this catalyst for dehydrocyclization is related to its low selectivity for hydrogenolysis, which may be, at least in part, a consequence of the smallness of the platinum clusters.

This is only the beginning in the investigation of supported metal clusters. Much remains to be learned about the structures, reactivities, and catalytic properties of these materials. Advancement of this understanding will require continued developments in characterization science and extension of synthetic methods to broaden the class of materials. Imaging methods may be crucial for the characterization. Preparation of well-defined metal clusters on planar supports should allow application of imaging techniques and many ultrahigh vacuum techniques, and one might anticipate that preparations from size-selected gas-phase clusters would allow investigation of variously sized clusters of a wide variety of metals. Further developments in EXAFS spectroscopy are also expected to be important.

Acknowledgments

This work was supported by the National Science Foundation (CTS-9300754).

References

(1) Anderson, J. R. *Structure of Metallic Catalysts*; Academic Press: New York, 1975.
(2) Boudart, M. *J. Mol. Catal.* **1985**, *30*, 27.
(3) Sinfelt, J. H. *Bimetallic Catalysts: Discoveries, Concepts, and Applications*; Exxon Monograph; Wiley: New York, 1983.
(4) Boudart, M. *Adv. Catal.* **1969**, *20*, 153.
(5) Boudart, M.; Djéga-Mariadassou, G. *Kinetics of Heterogeneous Catalytic Reactions*; Princeton University Press: Princeton, NJ, 1984.
(6) Poltorak, O. M.; Boronin, V. S. *Russ. J. Phys. Chem.* **1966**, *40*, 1436.
(7) Che, M.; Bennett, C. O. *Adv. Catal.* **1989**, *36*, 55.
(8) Somorjai, G. A.; Carrazza, J. *Ind. Eng. Chem. Fundam.* **1986**, *25*, 63.
(9) Muetterties, E. L. *Bull. Soc. Chim. Belg.* **1975**, *84*, 959.
(10) Kaesz, H. D. In *Metal Clusters in Catalysis*; Gates, B. C.; Guczi, L.; Knözinger, H., Eds.; Elsevier: Amsterdam, 1986.
(11) Shriver, D. F., Kaesz, H. D., Adams, R. D., Eds. *The Chemistry of Metal Cluster Complexes*; VCH: New York, 1990.
(12) Kaldor, A.; Cox, D. M. *J. Chem. Soc. Faraday Trans.* **1990**, *86*, 2459.
(13) Pan, Y. H.; Sohlberg, K.; Ridge, D. P. *J. Am. Chem. Soc.* **1991**, *113*, 2406.
(14) Schnabel, P.; Irion, M. P.; Weil, K. G. *J. Phys. Chem.* **1991**, *95*, 9688.
(15) Muetterties, E. L.; Krause, M. J. *Angew. Chem., Int. Ed. Engl.* **1983**, *22*, 135.
(16) Basset, J.-M.; Ugo, R. *Aspects Homogeneous Catal.* **1977**, *3*, 137.
(17) Chini, P. *Gazz. Chim. Ital.* **1979**, *109*, 225.
(18) Gates, B. C.; Lamb, H. H., *J. Mol. Catal.* **1989**, *52*, 1.
(19) Gates, B. C., Guczi, L., Knözinger, H., Eds. *Metal Clusters in Catalysis*; Elsevier: Amsterdam, 1986.
(20) Iwasawa, Y. *Catal. Today* **1993**, *18*, 21.
(21) Ichikawa, M. *Adv. Catal.* **1992**, *38*, 283.
(22) Gates, B. C. *J. Mol. Catal.* **1994**, *86*, 95.
(23) Hugues, F.; Basset, J.-M.; Ben Taarit, Y.; Choplin, A.; Primet, M.; Rojas, D.; Smith, A. K. *J. Am. Chem. Soc.* **1982**, *104*, 7020.
(24) Lamb, H. H.; Fung, A. S.; Tooley, P. A.; Puga, J.; Krause, T. R.; Kelley, M. J.; Gates, B. C. *J. Am. Chem. Soc.* **1989**, *111*, 8367.
(25) Kawi, S.; Gates, B. C. *Inorg. Chem.* **1992**, *31*, 2939.
(26) Pierantozzi, R.; Valagene, E. G.; Nordquist, A. F.; Dyer, P. N. *J. Mol. Catal.* **1983**, *21*, 189.
(27) Puga, J.; Patrini, R.; Sanchez, K. M.; Gates, B. C. *Inorg. Chem.* **1991**, *30*, 2479.
(28) Kawi, S.; Chang, J.-R.; Gates, B. C. *J. Phys. Chem.* **1993**, *97*, 5375.
(29) Roberto, D.; Psaro, R.; Ugo, R. *Organometallics* **1993**, *12*, 2292.
(30) Eberhardt, W.; Fayet, P.; Cox, D.; Kaldor, A.; Sherwood, R.; Sondericker, D. *Phys. Scr.* **1990**, *41*, 892.
(31) Roy, H. V.; Fayet, P.; Patthey, F.; Schneider, W. D.; Delly, B.; Massobrio, C. *Phys. Rev. B*, **1994**, *49*, 5611.
(32) Kawi, S.; Gates, B. C. In *Clusters and Colloids*; Schmid, G., Ed.; VCH: Weinheim, 1994; p 299.
(33) Sachtler, W. M. H.; Zhang, Z. *Adv. Catal.* **1993**, *39*, 129.
(34) Psaro, R.; Ugo, R.; Zanderighi, G. M.; Besson, B.; Smith, A. K.; Basset, J.-M. *J. Organomet. Chem.* **1981**, *213*, 215.
(35) Deeba, M.; Gates, B. C. *J. Catal.* **1981**, *67*, 303.
(36) Knözinger, H.; Zhao, Y. *J. Catal.* **1981**, *71*, 337.
(37) Psaro, R.; Dossi, C.; Fusi, A.; Ugo, R. *Res. Chem. Intermed.* **1991**, *15*, 31.
(38) Hsu, L.-Y.; Shore, S. G.; D'Ornelas, L.; Choplin, A.; Basset, J.-M. *J. Catal.* **1994**, *149*, 159.
(39) Krause, T. R.; Davies, M. E.; Lieto, J.; Gates, B. C. *J. Catal.* **1985**, *94*, 195.
(40) Xu, Z.; Kawi, S.; Gates, B. C. *Inorg. Chem.* **1994**, *33*, 503.
(41) Xu, Z.; Rheingold, A.; Gates, B. C. *J. Phys. Chem.* **1993**, *97*, 9465.
(42) Dossi, C.; Psaro, R.; Roberto, D.; Ugo, R.; Zanderighi, G. M. *Inorg. Chem.* **1990**, *29*, 4368.
(43) Kawi, S.; Chang, J.-R; Gates, B. C. *J. Phys. Chem.* **1993**, *97*, 10599.
(44) Kawi, S.; Chang, J.-R; Gates, B. C. *J. Am. Chem. Soc.* **1993**, *115*, 4830.
(45) Kawi, S.; Chang, J.-R; Gates, B. C. To be published.
(46) Xu, Z.; Xiao, F.-S.; Purnell, S. K.; Alexeev, O.; Kawi, S.; Deutsch, S. E.; Gates, B. C. *Nature (London)* **1994**, *372*, 346.
(47) van Zon, F. B. M.; Maloney, S. E.; Gates, B. C.; Koningsberger, D. C. *J. Am. Chem. Soc.* **1993**, *115*, 10317.
(48) Chang, J.-R.; Koningsberger, D. C.; Gates, B. C. *J. Am. Chem. Soc.* **1992**, *114*, 6460.
(49) Lamb, H. H.; Wolfer, M.; Gates, B. C. *J. Chem. Soc., Chem. Commun.* **1990**, 1296.
(50) Beutel, T.; Kawi, S.; Purnell, S. K.; Knözinger, H.; Gates, B. C. *J. Phys. Chem.* **1993**, *97*, 7284.
(51) Xiao, F.-S.; Alexeev, O.; Gates, B. C. *J. Phys. Chem.*, **1995**, *99*, in press.
(52) Jacobs, P. In *Metal Clusters in Catalysis*; Gates, B. C., Guczi, L., Knözinger, H., Eds.; Elsevier: Amsterdam, 1986; pp 357–414.
(53) Gallezot, P. *Catal. Rev.—Sci. Eng.* **1979**, *20*, 121.
(54) Gallezot, P. In *Metal Clusters*; Moskovits, M., Ed.; Wiley-Interscience: New York, 1986; pp 219–247.
(55) Dalla Betta, R. A.; Boudart, M. *Proc. 5th Int. Congr. Catal.* **1973**, *2*, 96–1329.
(56) Reagan, W. J.; Chester, A. W.; Kerr, G. T. *J. Catal.* **1981**, *69*, 89.
(57) Chester, A. W. *J. Catal.* **1984**, *86*, 16.
(58) Otten, M. M.; Clayton, M. J.; Lamb, H. H. *J. Catal.* **1994**, *149*, 211.
(59) Lane, G. S.; Modica, F. S.; Miller, J. T. *J. Catal.* **1991**, *129*, 145.
(60) Buss, W. C.; Hughes, T. R. UK Patent Application 2116450, 1983.
(61) Vaarkamp, M.; Grondelle, J. V.; Miller, J. T.; Sajkowski, D. J.; Modica, F. S.; Lane, G. S.; Gates, B. C.; Koningsberger, D. C. *Catal. Lett.* **1990**, *6*, 369.
(62) (a) Triantafillou, N. D.; Miller, J. T.; Gates, B. C. *J. Catal.*, submitted for publication. (b) Triantafillou, N. D.; Deutsch, S. E.; Alexeev, O.; Miller, J. T.; Gates, B. C. *J. Catal.*, submitted for publication.
(63) Rice, S. B.; Koo, J. Y.; Disko, M. M.; Treacy, M. M. J. *Ultramicroscopy* **1990**, *34*, 108.
(64) Cox, D. M.; Fayet, P.; Brickman, R.; Hahn, M. Y.; Kaldor, A. *Catal. Lett.* **1990**, *4*, 271.
(65) Koningsberger, D. C., Prins, R., Eds. *X-ray Absorption: Principles, Applications, Techniques of EXAFS, SEXAFS, and XANES;* Wiley: New York, 1988.
(66) Gates, B. C.; Koningsberger, D. C. *CHEMTECH* **1992**, *22*, 300.
(67) Maloney, S. D.; van Zon, F. B. M.; Koningsberger, D. C.; Gates, B. C. *Catal. Lett.* **1990**, *5*, 161.
(68) Kawi, S.; Chang, J.-R.; Gates, B. C. *J. Phys. Chem.* **1994**, *98*, 12978.
(69) Triantafillou, N. D.; Gates, B. C. *J. Phys. Chem.* **1994**, *98*, 8431.
(70) Asakura, K.; Iwasawa, Y. *J. Chem. Soc. Faraday Trans.* **1990**, *86*, 2657.
(71) Fung, A. S.; Tooley, P. A.; Kelley, M. J.; Koningsberger, D. C.; Gates, B. C. *J. Phys. Chem.* **1991**, *95*, 225.
(72) Zhang, Z.; Cavalcanti, F. A. P.; Sachtler, W. M. H. *Catal. Lett.* **1992**, *12*, 157.
(73) Lamb, H. H.; Wolfer, M.; Gates, B. C. To be published.
(74) Maloney, S. D. Ph.D. Dissertation, University of Delaware, 1990.
(75) Maloney, S. D.; Kelley, M. J.; Koningsberger, D. C.; Gates, B. C. *J. Phys. Chem.* **1991**, *95*, 9406.
(76) Churchill, M. R.; Hutchinson, J. P. *Inorg. Chem.* **1978**, *17*, 3528.
(77) Bau, R.; Chiang, M. Y.; Wei, C.-Y.; Garlaschelli, L.; Martinengo, S.; Koetzle, T. F. *Inorg. Chem.* **1985**, *23*, 4758.
(78) Demartin, F.; Manassero, M.; Sansoni, M.; Garlaschelli, L.; Martinengo, S.; Canziani, F. *J. Chem. Soc., Chem. Commun.* **1980**, 904.
(79) Vaarkamp, M.; Modica, F. S.; Miller, J. T.; Koningsberger, D. C. *J. Catal.* **1993**, *144*, 611.
(80) Miller, J. T.; Meyers, B. L.; Modica, F. S.; Lane, G. S.; Vaarkamp, M.; Koningsberger, D. C. *J. Catal.* **1993**, *143*, 395.
(81) Samant, M. G.; Boudart, M. *J. Phys. Chem.* **1991**, *95*, 4070.
(82) Rabo, J. A.; Schomaker, V.; Pickert, P. E. *Proc. 3rd Int. Congr. Catal.*; North Holland: Amsterdam, 1965; Vol. 2, p 1264.
(83) Sachtler, W. M. H. *Acc. Chem. Res.* **1993**, *26*, 387.
(84) Purnell, S. K.; Xu, X.; Goodman, D. W.; Gates, B. C. *J. Phys. Chem.* **1994**, *98*, 4076.
(85) Ravenek, W.; Jansen, A. P. J.; van Santen, R. A. *J. Phys. Chem.* **1989**, *93*, 6445.
(86) *Oil Gas J.* **1992**, *190*, 29.
(87) Rotman, D. *Chem. Week* **1992**, *150*, 8.
(88) Bernard, J. R. In *Proc. 5th Int. Zeolite Conf.*; Rees, L. V. C., Ed.; Heyden: London, 1986; p 686.
(89) Hughes, T. R.; Buss, W. C.; Tamm, P. W.; Jacobson, R. L. In *New Developments in Zeolite Science and Technology*; Murakami, Y., Iijima A., Ward, J. W., Eds.; Elsevier: Amsterdam, 1986; p 725.
(90) Larson, G.; Haller, G. L. *Catal. Lett.* **1989**, *3*, 103.
(91) Tamm, P. W.; Mohr, D. H.; Wilson, C. R. In *Catalysis 1987*; Ward, J. W., Ed.; Elsevier: Amsterdam, 1988; p 335.
(92) Mielczarski, E.; Hong, S. B.; Davis, R. J.; Davis, M. E. *J. Catal.* **1992**, *134*, 359.
(93) Besoukhanova, C.; Guidot, J.; Barthomeuf, D.; Breysse, M.; Bernard, J. R. *J. Chem. Soc., Faraday Trans.* **1981**, *77*, 1595.
(94) Han, W.-H.; Kooh, A. B.; Hicks, R. F. *Catal. Lett.* **1993**, *18*, 193.
(95) Han, W.-H.; Kooh, A. B.; Hicks, R. F. *Catal. Lett.* **1993**, *18*, 219.
(96) Miller, J. T.; Modica, F. S.; Meyers, B. L.; Koningsberger, D. C. *Prepr., Div. Petrol. Chem., Am. Chem. Soc.* **1993**, *38*, 825.
(97) Tauster, S. J.; Steger, J. J. *J. Catal.* **1990**, *125*, 387.

CR940094T